International Journal of Physical Sciences Vol. 7(12), pp. 1910- 1917, 16 March, 2012
Available online at http://www.academicjournals.org/IJPS
DOI: 10.5897/IJPS11.1743
ISSN 1992 - 1950 ©2012 Academic Journals

Full Length Research Paper

Absorbed Dose Estimation by Monte Carlo Simulation Conversion Factor of Physical Dosimeters

Yasser Saleh ALAJERAMI*, Suhairul HASHIM, Wan Muhamad Saridan WAN HASSAN and Ahmad Termizi RAMLI.

Department of Physics, Universiti Teknologi Malaysia, 81310 Skudai, Johor, Malaysia.

Accepted 30 January, 2012

In our world, nuclear accident is unavoidable. This means that we are under radiation risk all the time. Therefore, you should determine the ionized atoms (absorbed dose) punctually and as fast as possible to deal properly with victims in the triage process. The present study attempts to determine the absorbed dose generated in femur bone that utilized femur phantom (Health Physics Society N13.32) after different energy levels (30 keV to 10 MeV) relying on the numerical simulation of Monte Carlo N-Particle (MCNP)-5. The results showed the gradual reduction of Kerma air free values with the increase of energy from 30 to 100 keV, after a dramatic increase was noticed up to 10 MeV. The behaviour of the conversion factor illustrated the inverse relation with increment of energy. The first value was obtained at 30 keV (0.0368 Gy/Gy) and remarkable decrease was observed up to 150 keV (0.0245 Gy/Gy). The conversion factor remains almost constant between 200 and 800 keV and dramatic depression specified the higher energies. Further work suggestion is to estimate the conversion factors with plastic buttons and ribs bone or mediastinum, and between eye glasses with orbital tissue

Key words: Absorbed dose, dose conversion, Kerma free air, mass absorption coefficient, Monte Carlo simulation, radiation accident.

INTRODUCTION

The absorbed dose is an essential factor that is used to estimate the level of risk and damage that result from exposure to ionizing radiation. Unfortunately, our world is amenable to intended or unintended radiological accident at any time. During this accident, the dose received by victims is an important factor to be determined as soon as possible to obtain fast and effective triage process. Early and precise dose estimation allows a physician to establish and define the most appropriate therapy. Several methods are used for retrospective dose estimation (physically and biologically) to determine the severity of dose absorption. The electron paramagnetic resonance (EPR) or electron spin resonance (ESR) is one of the most successful techniques used in dose reconstruction after the radiation accident. The EPR can be observed in any substance containing at least one unpaired electron. Many studies investigate the sensitivity of EPR spectrometer to estimate the absorbed dose. These estimations can be classified into physical material estimation (plastic buttons, wrist watches, mobile phone, eye glasses, cotton and credit card) (Dalgarno and McClymont, 1989; Frantz et al., 2005; Bassinet et al., 2010) and biological materials estimation (bone, tooth, sugar, fingernail and hair) (Marrale et al., 2011; Romanyukha et al., 2007; Ghiani et al., 2008).

On the other hand, the EPR tends to measure the dose response from the sample, and then it must be converted into absorbed dose. Furthermore, the intended material, designed to be used as a retrospective dosimeter should be prepared in a specific method (sample preparation, grinding and temperature adjustment), and should be adjusted with certain protocol (sample position, magnetic

*Corresponding author. E-mail: Yasser_ajr@hotmail.com.

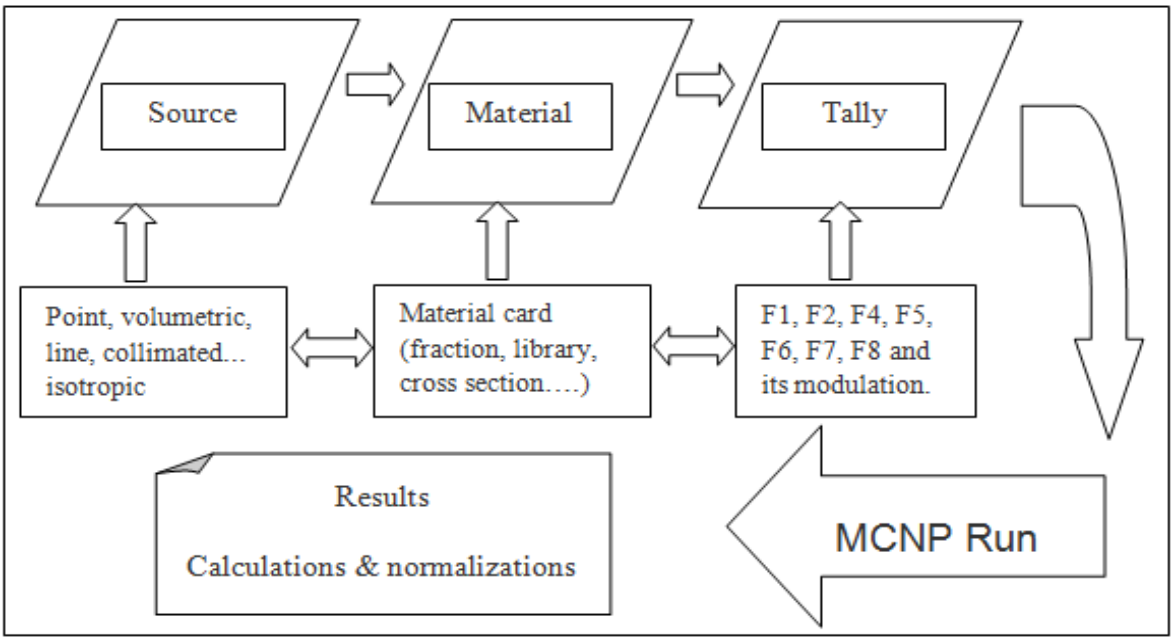

Figure 1. Overview on the main steps of MCNP simulation.

field and signal channel determination) in order to get punctual estimation of absorbed dose. All previous parameters and calibrations are time and cost consuming and they affect strongly the percentage of uncertainty. Therefore, all recent studies recommend the using of EPR spectrometer with other physical dose reconstructions by utilizing numerical means (Monte Carlo code simulations, mathematical calculations and/or voxel anthropomorphic phantoms) to confirm the estimations (Ghiani et al., 2008; Clairand et al., 2008). Moreover, the numerical estimation of the absorbed dose simplifies the determination of actual absorbed dose from the noise-induced signals (background and mechanical noise). The continuous integration of computer technology empowered the efficiency of simulation to calculate the absorbed dose at any point in the exposed target (Huet et al., 2007; Lemosquet et al., 2004). The present study aims to estimate the absorbed dose and dose conversion coefficient (DCC) in the range of 30 keV up to 10 MeV for the plastic holder of monitor display in mobile phone. The plastic is considered one of the most available, widespread and close materials to human body, and above all non-invasive to estimate with EPR combination. The simulations are performed by utilizing Monte Carlo N-Particle (MCNP^{TM}) code version 5 (V5).

MONTE CARLO SIMULATION

Nowadays, majority of physical experiments are jointed with mathematic or numerical calculations by using radiation transport code (Takahashi and Endo,and Yamaguchi 2007). In radiation protection and dosimetry, the simulation becomes one of the most significant tools that is used to assure the results obtained by experiments; particularly, in the process of absorbed dose determination after the radiation accident.

MCNP5 is one of the most powerful simulations that is widely used in medical physics. This code has the advantage of being documented and subjected to regular updates. Initially, MCNP is designed for calculation involving neutrons only. Then, it was subsequently generalized to the transport of photons and electrons in a wide energy range; finally, the positron was included during the coding of MCNP5. Currently, MCNP^{TM} code version 5 (V5) provides continuous-energy, generalized-geometry, time-dependent code and can be used for single, couple or more of neutron/photon/electron transport. One main difference of MCNP from other Monte Carlo codes is that MCNP can be run in several different modes. By default, mode N is used; neutron transport only (X-5 MC Team, 2005).

Figure 1 shows the three main steps that should be followed carefully to get precise simulation; source specification, target and tally determination. Figure 1 illustrates the process of particle tracks and its interaction with the materials, according to probability density distributions attained by particle and material properties.

Source specification

In this simulation, the user specified the SDEF command to specify the material card in the input file. The radiation source was assumed as a monodirectional point source, and the photons were emitted uniformly from a cone direction. The source and the geometrical target of plastic goods were separated with a distance of 100 cm. All simulations were performed inside a sphere with 120 cm diameter, and the space between the spherical surface and the target was considered as dry air (D = 1.205 × 10^{-3} g/cm^3). The particles were confined to a downward (-z axis) cone whose half-angle is a cosine of the solid angle about the z-axis. The source angles were determined with respect to the vector (VEC) and direction (DIR). The source information entries were determined according to the specified target to ensure that the entire sample

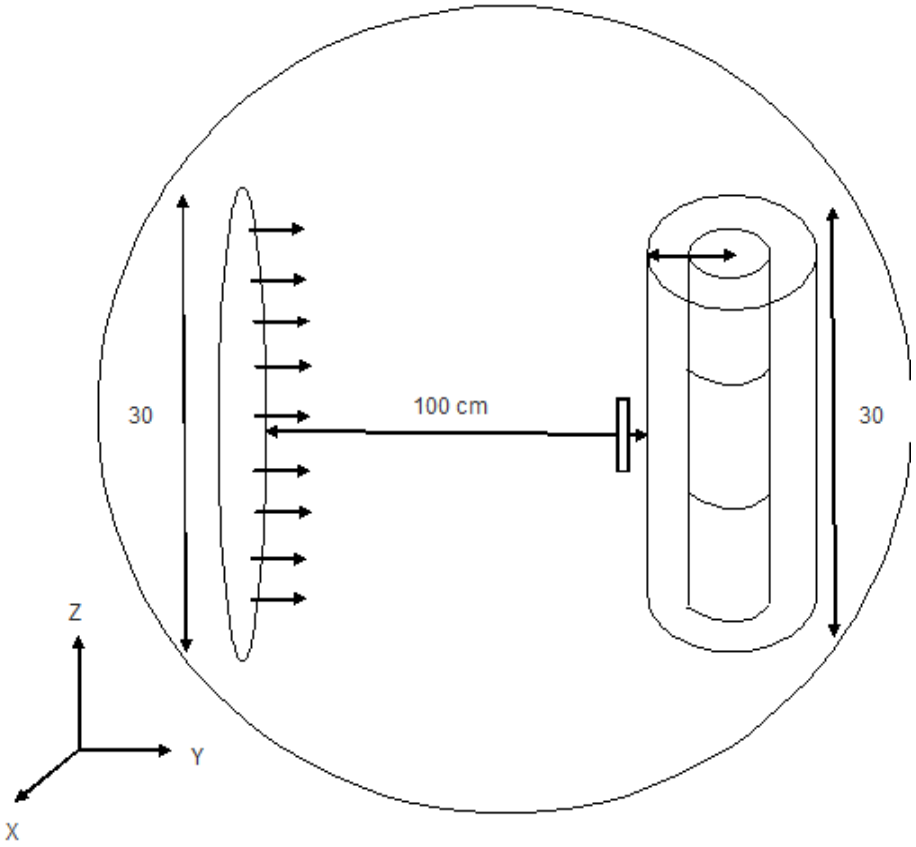

Figure 2. Extermity phantom model according to the ICRP/MIRD and ANSI/HPS N13.32 with small modifications. (Cylinder with 4.5 cm for outer radius and 3 cm for inner radius; 30 cm height and soft tissue and bone compositions).

was uniformly covered as shown in Figure 2. Consequently, the most appropriate type is the disk source. The disk source was assumed with a radius of 15 cm with parallel radiation beam.

Target determination

Five plastic holders (mobile monitor display) from different brand were selected to be a retrospective dosimeter, and were used to determine the absorbed dose and dose response after radiation accident. Scanning electron microscope (SEM) technique was used to determine the fractional molecular weight, and consequently to measure the relative elemental composition of the plastic holders. Table 1 demonstrates the chemical compositions of each plastic goods with their densities. Previous studies confirm the efficiency of hydroxyapatite ($C_{10}(PO_4)_6(OH)_2$) contained in bones (>70%) and teeth (>95%) as a probe for ionizing radiation; particularly, its stability in room temperature. During this study, conversion calculations were measured to estimate the conversion factor between the plastic cover of mobile phone to the femur bone.

To facilitate the process of geometric modeling, researchers used the MCNP Visual Editor Version 19L-Vised22. The elementary compositions and densities of assigned organs were earned from No. 46 report of International Commission on Radiation Units and Measurements (ICRU). The assumed diameters were obtained from International Commission on Radiological Protection (ICRP/MIRD-phantom) and ANSI/HPS N13.32 (1995) with simple modifications, such as the replacement of aluminum with the human bone tissue, and the human soft tissue instead of polymethylmethacrylate (PMMA).

Phantom was defined as two right-circular cylinders. According to the ICRU reports No. 47, 51 and 57 (ICRU, 1992, 1993, 1998), tallies were performed at a depth of 0.07 mm within the extremity phantom described in HPS (Health Physics Society) N13.32, For weakly penetrating radiation, the ambient and directional dose equivalents in the skin at d = 0.07 mm, $H^*(0.07)$ and $H¢(0.07,W)$, are relevant, and in the eye lens at d = 3 mm, $H^*(3)$ and $H¢(3,W)$, are relevant.

Tally determination

The process of tally specification means what type of data the user needed to obtain the simulation. In the present study, researchers determined the absorbed dose of different plastic goods by *F8 and the Kerma free air was determined by applying *F4. The absorbed dose can be measured by *F4, *F6 and *F8, but the closet tally for physical detectors is *F8 (record the deposited energy from incident particle and its secondary particles). During theses simulations, researchers used the non-analogous code with source biasing by starting the particles in preferred directions, generally toward specified target (Tally regions). Several termination steps were used to minimize the relative errors and variance of variance (less than 2%); the number of histories (NPS) for each simulation exceeded the 5×10^7 (to achieve high accuracy and statistical error around less than 2% for each simulation); the geometries were

Table 1. Atomic, weight fractions and densities of mobile phone covering holder examined in the present study.

Plastic material	Covering holder 1	Covering holder 2	Covering holder 3	Covering holder 4	Covering holder 5
Weight fraction	H:0.05550 C:0.59985 O:0.31956	H:0.50525 C:0.20212 O:0.29262	H:0.62142 C:0.28961 O:0.08897	H:0.35356 C:0.54321 O:0.10323	H:0.48972 C:0.33341 O:0.17687
Density (g/cm^3)	1.19	1.22	1.34	1.41	1.32

simplified; finally, we utilized the CUT-OFF to kill the photon with energy below 1 keV (Briesmeister, 1997).

Absorbed dose estimation

The absorbed dose was determined by numerical simulation and the energy value was retrieved from *F8 tally converted to joule unit and normalized to the target's mass to get the absorbed dose per particle at each simulation.

$$D(Em) = \frac{retrived\ value\ (MeV)\ x\ 1.6x10E-13(Joule)}{mass\ (kg)} \quad (1)$$

The value revealed by the simulation is normalized by the number of particle.

Kerma free air

Based on report No. 47 of ICRU (ICRU, 1998), the Kerma free-in-air for monoenergetic photon beams was used to obtain the dose conversion coefficients according to the following formula:

$$\frac{Ka}{\Phi} = 160.22\ x\ \frac{\mu tr}{p}\ x\ E_{inc} \quad (2)$$

where $\frac{Ka}{\Phi}$ is the ratio of Kerma free-in-air to photon fluence, $\frac{\mu tr}{p}$ is the mass energy transfer coefficient and E_{inc} is the incident energy.

Dose conversion coefficient

The dose conversion ratio is a very important factor that set the difference between organ doses to measurable quantities. Based on this value, we can specify the dose (organ absorbed dose to physical dosimeters absorbed dose) received from different external sources (Trompier et al., 2011). The purpose of absorbed dose conversion coefficient calculation in this study is to confirm the accuracy of simulation by comparing our results with the results obtained by Vienot and Hertel (2007) (Figure 3). The conversion coefficients air Kerma was calculated using F6 tall with MCNP-5 by designing a rectangular solid air outside the phantom with equal diameter of 1 cm.

RESULTS AND DISCUSSION

Before starting the simulation, the users checked the validity of the design and input data (cell, surface and data card) with the Vised Window. Furthermore, a series of statistical parameters were also defined; the statistical uncertainty in the Monte Carlo calculation was smaller than 2% (2σ). All simulation processes passed the ten statistical checks. The relative errors and the variance of variance were decreased with increasing number of particles. The slope of a fluctuation chart was more than five. Figure of Merit (FOM) was almost constant in all the running steps. All previous parameters gave good indicators about the precision of our simulations.

The fractions compositions of the five mobile phones (holding cover) were analyzed by using SEM. The results are shown in Table 1. The mass energy absorption coefficient of each sample was calculated by the sum of $\left(\frac{\mu_{en}}{\rho}\right)_m$ taken from the value published by Hubbell and Seltzer (1995). Table 2 shows the mass energy absorption coefficient measured from 20 keV up to 10 MeV. A remarkable reduction was shown with the increase of energy. Table 3 illustrates the calculated air Kerma conversion coefficients for the femur bone. The current coefficients were compared with those done by Vienot and Hertel (2007).

Obviously, a great harmonization appeared between the calculated conversion coefficients of the current study and those determined by Vienot and Hertel (2007). This is another good indicator about the precision of our simulations. The results showed the gradual reduction of Kerma air free values with increasing energy from 30 to 100 keV, after that, a dramatic increase was noticed up to 10 MeV. This behavior is attributed to the predominant of photoelectron cross section at the low energy levels. The same table listed the absorbed dose conversion coefficients (calculated the air absorbed with 100 cm distance between the source and phantom).

The deposited energies (height tally) in a specific part of femur bone (10 cm height and diameter = 6 cm) were as shown in Table 4. The deposited energies gradually increased with lifting up of energies; however, this increase was slower in level above 1 MeV (Figure 4). The deposited energies were normalized at each energy level with mass of bone sample and the numbers of particles utilized in each running. The same calculations were repeated with five samples. All plastic dosimeters were designed to be outside the proposed phantom HPS N13.32 (2 cm from the skin surface). The energy

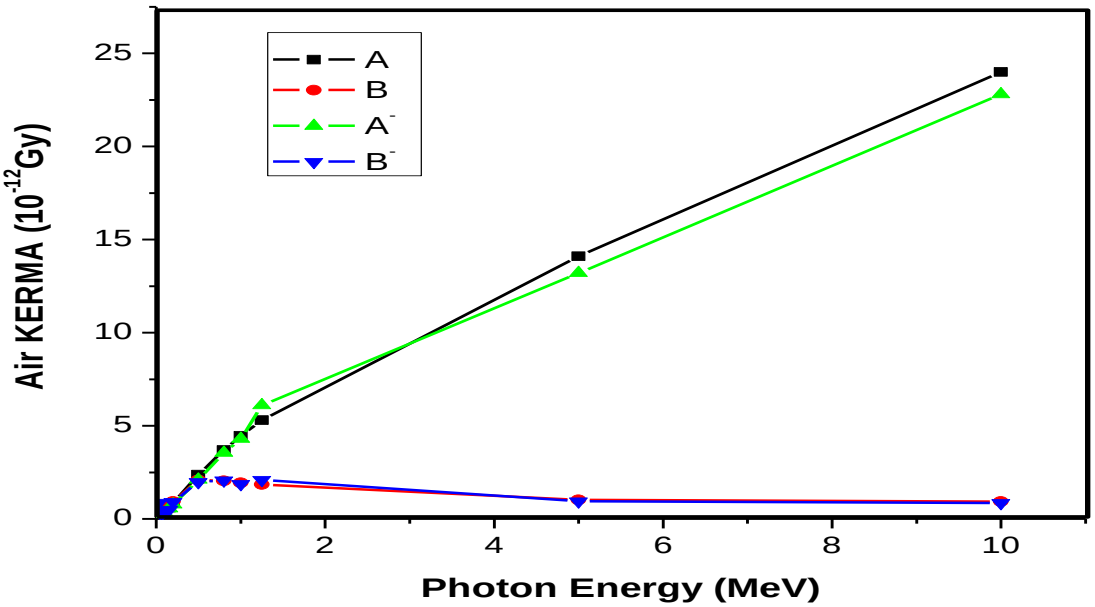

Figure 3. Comparison between the air-kerma-to-absorbed dose conversion coefficients during this study and Vienot and Hertel (2007). (A^-: Air kerma; B^-: 100 cm air absorbed dose of our study; A: Air kerma; B: 100 cm air absorbed dose of Veinot and Hertel (2007).

Table 2. Mass energy absorption coefficients.

Target	0.03	0.05	0.1	0.15	0.2	0.5	0.6	1	1.25	3	6	10
Bone	0.566	0.128	0.0346	0.0295	0.0407	0.0319	0.0317	0.0299	0.0286	0.0221	0.0178	0.0158
Air	0.1537	0.04098	0.02325	0.02496	0.02672	0.02966	0.02953	0.02789	0.02666	0.02057	0.01647	0.01405
Sample 1	0.0960	0.0300	0.0227	0.0254	0.0274	0.0306	0.0304	0.0288	0.0275	0.0211	0.0166	0.0143
Sample 2	0.0734	0.0314	0.0318	0.0366	0.0398	0.0445	0.0443	0.0419	0.0400	0.0304	0.0228	0.0185
Sample 3	0.0461	0.0277	0.0336	0.0392	0.0427	0.0479	0.0477	0.0451	0.0431	0.0326	0.0242	0.0193
Sample 4	0.0604	0.0272	0.0285	0.0329	0.0358	0.0401	0.0399	0.0377	0.0360	0.0274	0.0207	0.0170
Sample 5	0.0618	0.0291	0.0312	0.0362	0.0393	0.0440	0.0439	0.0415	0.0396	0.0300	0.0225	0.0182

Table 3. Calculated photon dose equivalent conversion coefficients for the femur phantom.

Photon energy (MeV)	Venot et al. (2007)		This study	
	Air Kerma (pGy cm^{-2}) F6	100 cm air absorbed dose (pGy cm^{-2}) F8	Air Kerma (pGy cm^{-2}) F6	100 cm air absorbed dose (pGy cm^{-2}) F8
0.03	0.67	0.70	0.54	0.87
0.05	0.31	0.33	0.29	0.31
0.08	0.30	0.35	0.29	0.33
0.1	0.37	0.41	0.31	0.45
0.15	0.60	0.68	0.55	0.50
0.2	0.85	0.93	0.77	0.91
0.5	2.37	2.09	2.11	1.99
0.8	3.69	2.04	3.55	2.08
1	4.46	1.94	4.30	1.88
1.25	5.30	1.84	6.1	2.1
5	14.1	1.02	13.2	0.95
10	24.0	0.93	22.8	0.85

All values were converted to Fluence per unit area by multiplying them with the area of source (706.86 cm^2).

Table 4. Values of deposited energy (*F8) of mobile covering holder (simulation values).

Values	0.03	0.05	0.08	0.1	0.15	0.2	0.5	0.8	1	1.25	5	10
***RSDE**	8.01786E-04	8.21906E-04	9.21006E-04	1.91404E-03	2.31336E-03	3.61736E-03	5.91726E-03	6.28916E-03	7.18103E-02	7.96E-02	7.99E-02	7.99E-02

*Relative samples deposit energy (normalized to sample mass).

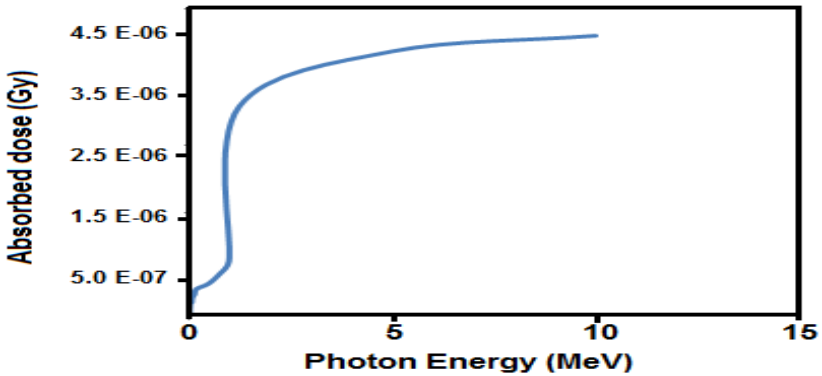

Figure 4. The relation between absorbed dose in femur bone and energy variations.

Table 5. Conversion factor between the absorbed dose in bone and average absorbed dose of mobile phone covering holders.

Factor	0.03	0.05	0.08	0.1	0.15	0.2	0.5	0.8	1	1.25	5	10
*NBAD	1.33E-08	1.62E-07	1.71E-07	2.50E-07	2.91E-07	3.70E-07	4.50E-07	6.11E-07	7.87E-07	3.06E-06	3.87E-06	4.10E-06
Conversion factor	3.68E-02	3.68E-02	3.66E-02	3.52E-02	2.45E-02	1.17E-02	1.11E-02	1.11E-02	8.01E-03	7.22E-04	7.21E-04	7.21E-04

*NBAD: Normalized bone absorbed dose (normalized to 10 cm mass of bone sample).

deposited in the covering holders were calculated to determine the dose conversion factor as shown in Table 5.

Figure 5 shows the conversion factors obtained between the average absorbed dose of five mobile phones covering holders and the absorbed dose in the femur bone (compact, cortical and cortex tissue). The behavior of the conversion factor illustrates the inverse relation with increment of energy. The first value obtained at 30 keV was 0.068 Gy/Gy, then a remarkable reduction was observed at 150 keV (0.0245 Gy/Gy). The conversion factor remains almost constant between 200 and 800 keV, and dramatic depression was specified at the higher energies.

Conclusion

Based on our review, it is the first study applied to determine the bone absorbed dose based on the

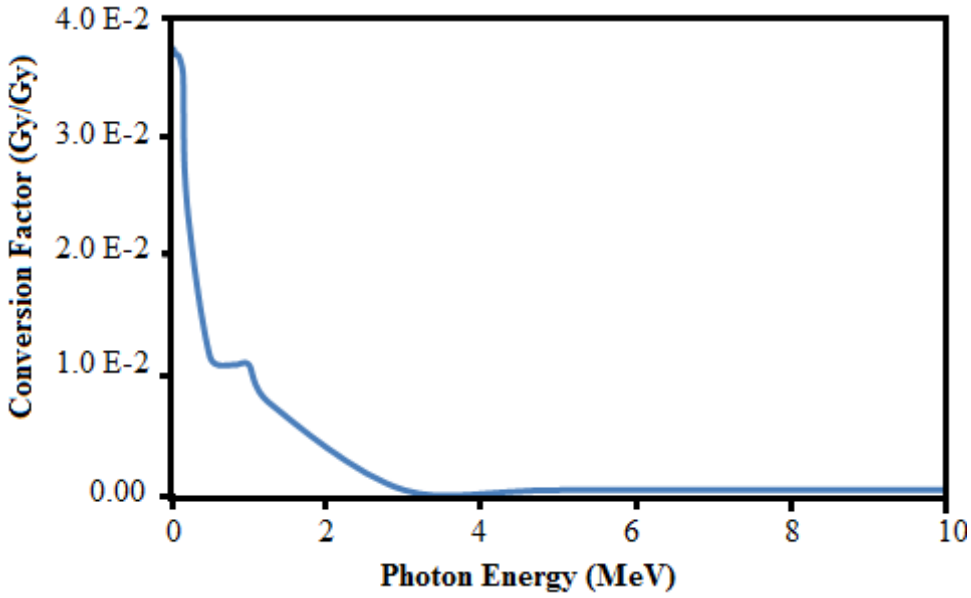

Figure 5. The conversion factors between the femur absorbed dose and relative absorbed dose of five mobile phone covering holders.

conversion factor plastic items. The calculation of absorbed dose in femur bone relies on the dose conversion factor of a plastic used to facilitate the process of dose estimation after the radiation accident. We can summarize our results into two main points. Firstly, the conversion factor was minimized with the increase of energies, and this means that the gap between the bone and plastic holders was increased with the increase of energy. Consequently, the absorbed dose in plastic covers was almost saturated with the low energy levels (30 to 80 keV) synchronizing with high probability of absorbed dose in femur bone at this level. Even though, the simulations in this study displays high precision and agreement with other simulations, the experimental work is highly recommended, particularly for non-invasive techniques. Finally, it is very appropriate to utilize the numerical simulation to estimate the absorbed dose in critical organs (bone) and conjunct with EPR for non-invasive materials located close to the human body (plastic buttons, eyeglass, wristwatches and others). Nevertheless, the success of the current idea, is very important to develop new procedures to estimate the absorbed dose with fast and simple way. Future work suggestion is to estimate the conversion factors with plastic buttons and ribs bone or mediastinum, and between eye glasses with orbital tissue.

ACKNOWLEDGEMENTS

The authors are very much thankful to Prof. Francois Tropmier and Sergey Sholom for their kind help to finish the current work. They are also grateful to UTM, for the preparation of equipment, the Ministry of Higher Education (MOHE) and The Ministry of Science, Technology and Innovation (MOSTI) and Universiti Teknologi Malaysia (UTM) for providing financial assistance through Research University Grant Scheme (RUGS), Project Number (Q.J130000.7126.01H60). Physically-based biodosimetry detected by electron paramagnetic resonance (EPR) for radiation accident emergency management.

REFERENCES

Bassinet C, Trompier F, Clairand I (2010). Radiation accident dosimetry on glass by Tl and Epr spectrometry. Health Phys., 98: 400-405.

Briesmeister JF (ed) (1997). MCNP - A general Monte Carlo n-p particle transport code version 4B. Los Alamos Laboratory Report LA-12625-M (Los Alamos, NM: Los Alamos National Laboratory).

Clairand I, Huet C, Trompier F, Bottollier-Depois JF (2008). Physical dosimetric reconstruction of a radiological accident due to gammagraphy equipment that occurred in Dakar and Abidjan in summer. Radiat. Meas., 43: 698-703.

Dalgarno BG, McClymont JD (1989). Evaluation of ESR as a radiation accident dosimetry technique. Appl. Radiat. Isot., 40: 1013–1020.

Frantz S, Hubner A, Wendland O, Roduner E (2005). Effect of humidity on the supramolecular structure of cotton, studied by quantitative spin probing. J. Phys. Chem. Ser. B, Mater. Surf. Interf. Biophys., 109(23): 11572-11579.

Ghiani S, Baroni S, Burgio D, Digilio G, Fukuhara M, Martino P, Monda K, Nervi C, Kiyomine A, Aime S (2008). Characterization of human hair melanin and its degradation products by means of magnetic resonance techniques. Magn. Reson. Chem., 46(5): 471-479.

Hubbell JH, Seltzer SM (1995). Tables of X-Ray Mass Attenuation Coefficients and Mass Energy-Absorption Coefficients 1 keV to 20 MeV for Elements Z _ 1 to 92 and 48. Additional Substances of Dosimetric Interest." Report NISTIR 5632 (Gaithersburg, MD: National Institute of Standards and Technology), pp. 33: 1269-1275.

Huet C, Clairand I, Trompier F, Bey E, Bottollier-Depois JF (2005).

Monte Carlo dose reconstruction in case of a radiological accident: Application to the accident in Chile in December, Radioprotection, 42: 489–500.
International Commission on Radiation Units and Measurements (1992). Measurement of dose equivalents from external photon and electron radiations. Bethesda, MD: ICRU Publication, p. 47.
International Commission on Radiation Units and Measurements (ICRU) (1993). Quantities and units in radiation protection dosimetry. Bethesda, MD: ICRU Publication, p. 51.
International Commission on Radiation Units and Measurements (1998). Conversion coefficients for use in radiological protection against external radiation Bethesda, MD: ICRU Publication, p. 57.
Lemosquet A, Clairand I, Carlan L, Franck D, Aubineau-Laniece I, Bottollier-Depois JF (2004). A computational tool based on voxel geometry for dose reconstruction of a radiological accident due to external exposure. Radiat. Prot. Dosim., 110: 449–454.
Marrale M, Longo A, D'Oca M.C, Bartolotta A, Brai M (2011). Watch glasses exposed to 6 MV photons and 10 MeV electrons analysed by means of ESR technique: A preliminary study. Radiat. Meas., 46: 822-826.
Romanyukha A, Mitchell CA, Schauer DA, Romanyukha L, Swartz HM (2007). Q-band EPR biodosimetry in tooth enamel microsamples: Feasibility test and comparison with X-band. Health Phys., 93: 631–635.
Takahashi F, Endo A (2007). Numerical system utilizing a Monte Carlo calculation method for precise dose assessment in radiation accidents. Radiat. Prot. Dosim, 126: 595–599.
Trompier F, Della Monaca S, Fattibene P (2011). EPR dosimetry of glass substrate of mobile phone LCDs. Radiat. Meas., 32: 827-831.
Veinot KG. Hertel NE (2007). Photon Extremity Absorbed Dose and Kerma Conversion Coefficients for Calibration. Health Phys., 92(2): 179-185.